Temporal coherence in particulate matters in East Asian outflow regions: fingerprints of ENSO, Asian dust and COVID-19

Mien-Tze Kueh[1], Chuan-Yao Lin[*1] & Yi-Yun Chien[1]
[1]Research Center for Environmental Changes, Academia Sinica, Taipei, Taiwan
[*]Corresponding author (Email: yao435@rcec.sinica.edu.tw)

Contents of this file:

Supplementary materials for

(A) standardization and exceedance frequency
- Supplementary Table 1
- Supplementary Figs. 1 to 3

(B) ENSO event and proportion of exceedance frequency
- Supplementary Table 2

(C) dust association
- Supplementary Figs. 4 to 5
- Supplementary Table 3

(A) Standardization and exceedance frequency

Supplementary Table 1 The long-term means (AVG), standard deviations (SD), and 90th percentiles of cold season for each site. *NA* denotes not applicable. To identify potential coherent patterns, a threshold for PM exceedance is determined using one standardized anomaly (1SD). A daily PM level > AVG+(1xSD) meet the 1SD threshold for PM exceedance calculation, and ACG+(2xSD) for the 2SD. The values of 90th percentiles for EANET sites are shown for a comparison.

	$PM_{2.5}$			PM_{10}		
	AVG	SD	90th	AVG	SD	90th
TW	32.89	20.67	*NA*	65.78	37.27	*NA*
HK	27.84	18.52	*NA*	48.17	28.86	*NA*
CNA008	*NA*	*NA*	*NA*	56.98	34.50	*NA*
JPA001	8.08	5.77	15.8	16.61	15.51	34.5
JPA004	9.37	5.83	16.8	22.77	17.85	41.9
JPA005	5.69	4.94	10.8	11.30	11.45	21.7
JPA006	8.64	5.60	15.9	18.89	14.65	29.7
JPA007	12.87	8.01	23.6	28.38	22.22	52.2
JPA009	9.89	6.31	18.4	17.11	14.60	33.1
JPA010	10.38	5.42	19.3	31.02	20.83	54.9
JPA011	6.11	3.76	11.7	13.91	9.38	25.5

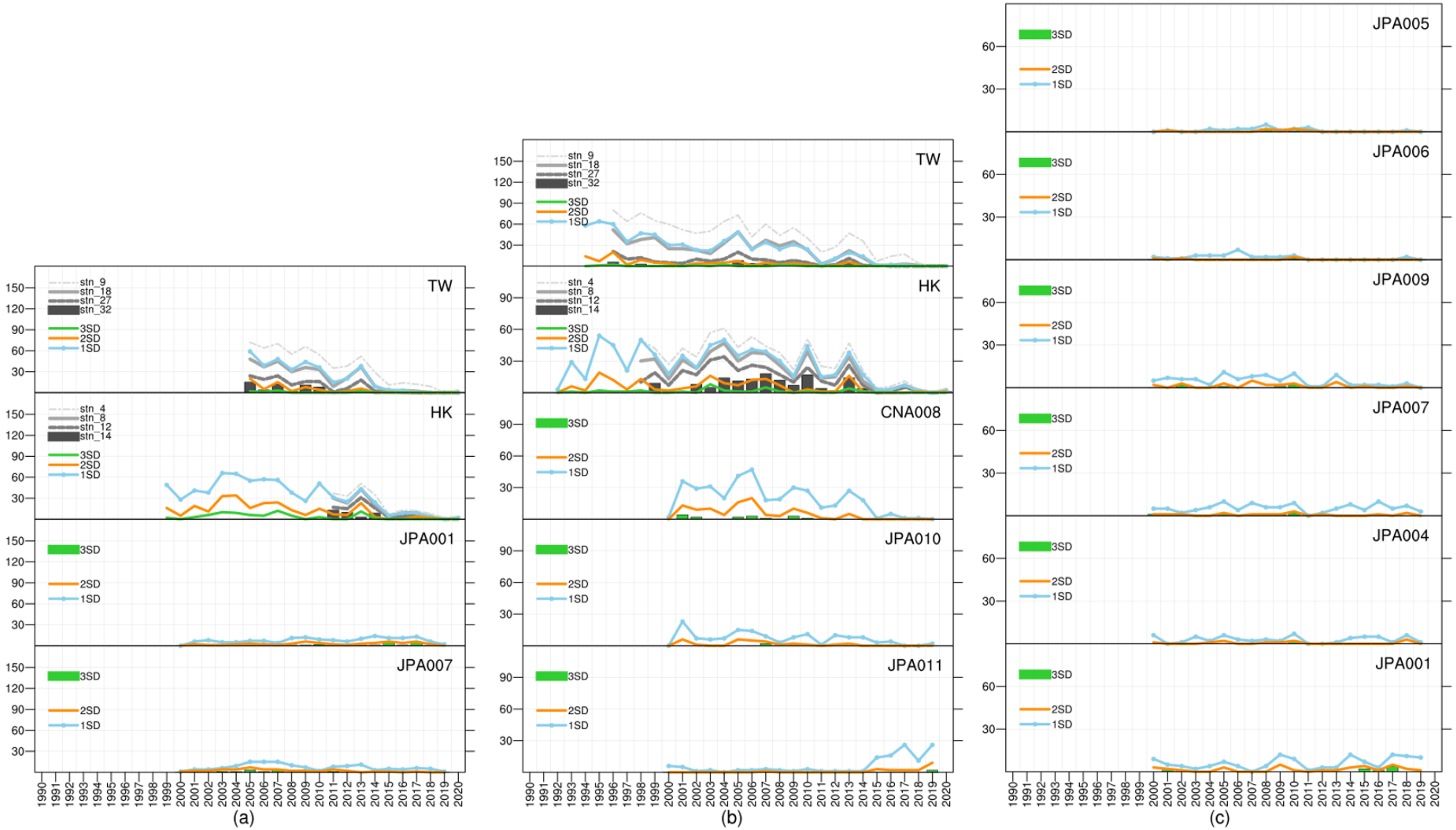

Supplementary Fig. 1. Temporal variations of daily PM exceedance frequencies for winter season. The exceedance frequency of $PM_{2.5}$ (**a**) and PM_{10} (**b** and **c**) derived from ground-based measurements for winter season (November to January). Y axis is numbers of day, X axis shows the years of the first month in the cold season. Each site has three sets of exceedance frequencies, which employ one, two, and three standardized anomalies as the thresholds for calculation, and denoted as 1SD, 2SD, and 3SD, respectively. Code names with prefixes JPA and CNA are for Japan and China, respectively. The exceedance frequencies of Taiwan (TW) and Hong Kong (HK) were derived from their respective daily mean values of selected stations. For TW and HK, additional sets of exceedance frequency were derived using the numbers of stations exceeding one standardized anomaly (1SD) as thresholds; the legends with prefix stn followed by a number indicates the number of stations used in the concurrence calculation.

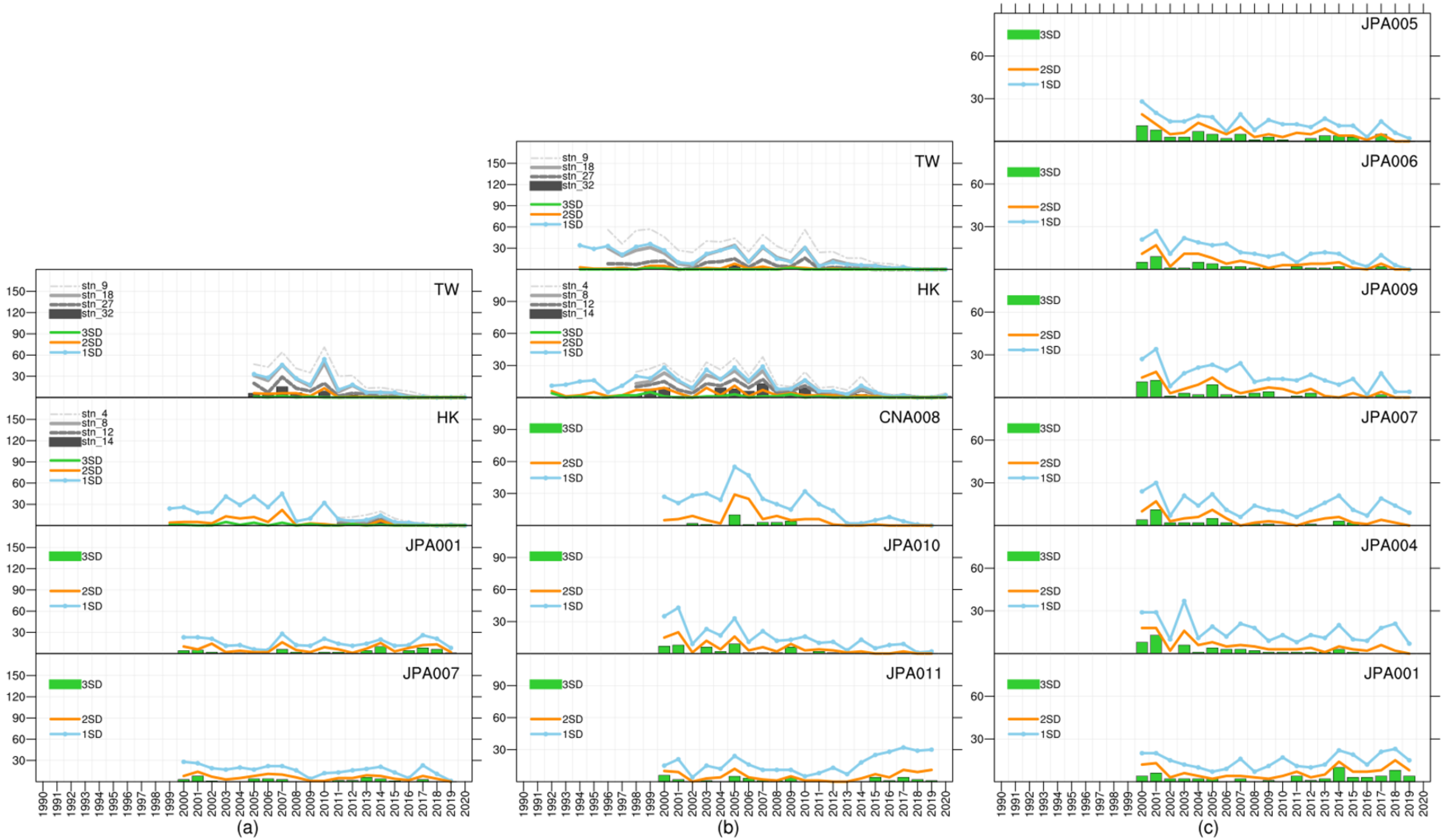

Supplementary Fig. 2. Temporal variations of daily exceedance frequencies for spring season. The same as in Fig. 1, but for spring season (February to April).

36

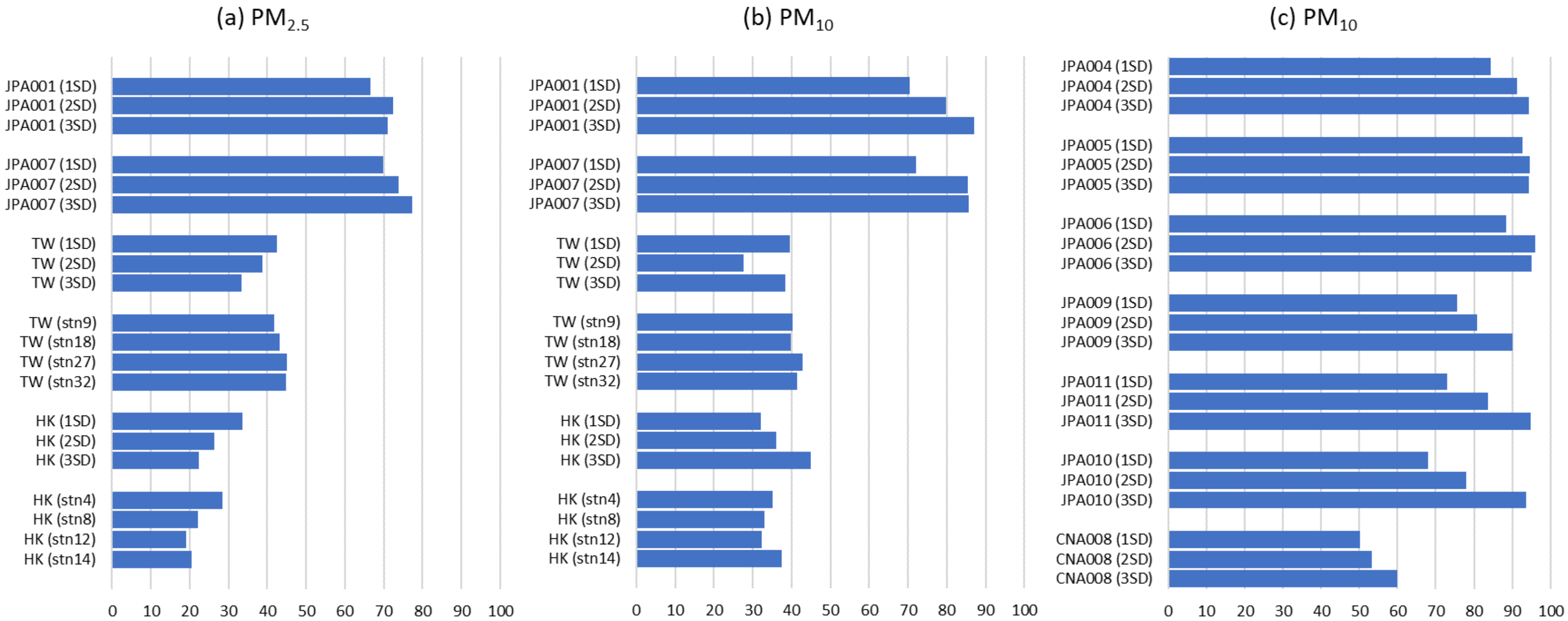

Supplementary Fig. 3. Contribution of springtime occurrences to the overall in cold season. Spring is from February to April; cold season is November to April.

(B) ENSO event and proportion of exceedance frequency

Supplementary Table 2 The proportion of occurrence of PM exceedance during El Niño (ONI+) and La Niña (ONI–) events in winter (NDJ) and spring (FMA). The significance (*p-value*) and data availability (expressed as percentage) are also listed.

			$PM_{2.5}$				PM_{10}										
			HK	TW	JPA007	JPA001	HK	TW	CNA008	JPA010	JPA011	JPA009	JPA007	JPA006	JPA005	JPA004	JPA001
Proportion of Occurrence (%)	NDJ	ONI –	22.20	13.82	9.73	8.75	19.25	16.61	12.35	5.15	5.44	5.13	2.80	2.02	2.07	2.62	5.82
		ONI +	21.27	18.79	7.04	8.95	17.08	12.73	15.06	4.67	4.10	2.96	1.60	2.64	0.92	1.91	6.88
	FMA	ONI –	12.96	14.24	19.90	18.30	12.48	14.40	19.94	16.67	15.85	16.67	10.95	17.44	19.52	14.72	12.00
		ONI +	8.65	9.78	17.74	15.14	7.85	5.29	12.92	7.25	15.76	14.26	8.83	15.06	14.89	10.67	15.10
Significance	*p-value*	NDJ	0.685	0.016	0.099	0.906	0.312	0.049	0.173	0.701	0.265	0.049	0.145	0.463	0.115	0.402	0.454
		FMA	0.014	0.015	0.35	0.142	0.007	7E-08	9E-04	4E-07	0.966	0.256	0.231	0.255	0.045	0.033	0.111
Data Availability (%)	NDJ	ONI –	100.00	100.00	81.37	83.39	100.00	100.00	89.29	84.47	97.05	99.84	99.69	99.84	89.91	94.72	88.04
		ONI +	100.00	100.00	97.05	98.91	100.00	100.00	97.98	99.84	98.45	99.53	97.05	100.00	84.16	97.36	99.38
	FMA	ONI –	100.00	100.00	91.68	97.92	100.00	100.00	99.52	99.84	90.88	98.88	87.68	100.00	86.88	98.88	100.00
		ONI +	100.00	100.00	92.15	94.23	100.00	100.00	99.20	97.28	99.68	88.78	94.39	100.00	83.97	97.60	98.72

(C) Dust association

In order to establish the connection between specific dates and dust activity, we employed a combination of data from the dust weather visual report, defined by World Meteorological Organization's SYNOP codes, and existing literature. The following procedures were followed:

1. We collected dust weather reports from available weather stations within our studied domain (90°–150°E, 20°–55°N) for the 57 dates of interest, as well as the 5 days prior to each date. The spatial distribution of these stations is shown in supplementary Fig. 4a, denoted with the highest dust code reported on specific station during our studied period.
2. The weather stations were then mapped onto a regular 1°x1° grid. We identified the grid cells that contained at least one weather station, marking them as dust cells (supplementary Fig. 4b).
3. From the selected dust cells, we processed the dust codes, categorizing them into continental and oceanic groups (supplementary Fig. 4c).
    a. Dusty level for each station: the maximum dust-related code within a day. (Weather codes are reported on 1-h, 3-h, 6-h, or 12-h intervals)
    b. Dusty level for each cell: the maximum code level found in the available weather station(s) within the target 1°x1° cell.
    c. Here, the calendar day is based on a UTC offset of UTC+8. For each calendar day, we counted the cell numbers of the dusty levels in each sub-region as an indicator. This indicator serves as a semi-objective complement in determining the occurrence of a dust episode.
    d. The dust codes used here includes widespread dust in suspension in the air (ww = 06), dust or sand raised by wind (ww = 07), dust or sand whirls (ww = 08), and dust or sand storms (ww = 09, 30–35, 98) at or near the station. Because there are less dust codes reported in the southern oceanic region, we added in two codes: Visibility reduced by smoke, e.g. veldt or forest fires, industrial smoke or volcanic ashes (ww = 04) and Haze (ww = 05).
    e. These weather codes are described in the WMO Code Table 4677.
    f. We do not have the weather reports for 2018.
4. By analyzing these dust codes, we were able to identify dates that were related to dust events.

a. Supplementary Table 3 outlined the result. Find details in the Table caption.

b. We have identified 3 types of dates (D_A, D_B, and D_r) that related to dust activities over East Asia, all termed as dust-related in the main text. D_A and D_B are cases with at least 10 dust cells and there were dust cell(s) found over the continental regions on the concurrent dates; D_r are cases with some dust cells on the concurrent dates and during the preceding few days.

5. Subsequently, we cross-referenced these dates with previously documented dust events in the available literature.
   a. All of the literature selected for analysis focused on Asian dust activity and explicitly provided dates for the investigated dust events.
   b. Each literature source was associated with a concurrent date if the date fell within the specified duration or within one day before or after the given period mentioned in the literature.
   c. The South Korean monitoring sites were excluded from the concurrent date calculation due to their limited availability of daily data over a short time range. However, it is worth noting that Asian dust events that impacted Japan also generally affected South Korea [1, 2, 3, 4, 5, 6, 7, 8, 9, 10] [11, 12, 13].
   d. Not all of the literature we encountered was included in our analysis.
   e. Some satellite-based images provided by the NASA Earth Observatory were also used as complementary materials.

In total, we have obtained 30 D_A, 10 D_B, and 11 D_r. All 30 D_A can be associated with existing literature. For D_B and D_r, both have 7 dates can be associated with existing literature. As for the rest 5 dates, we were unable to determine the type based on dust codes and literature.

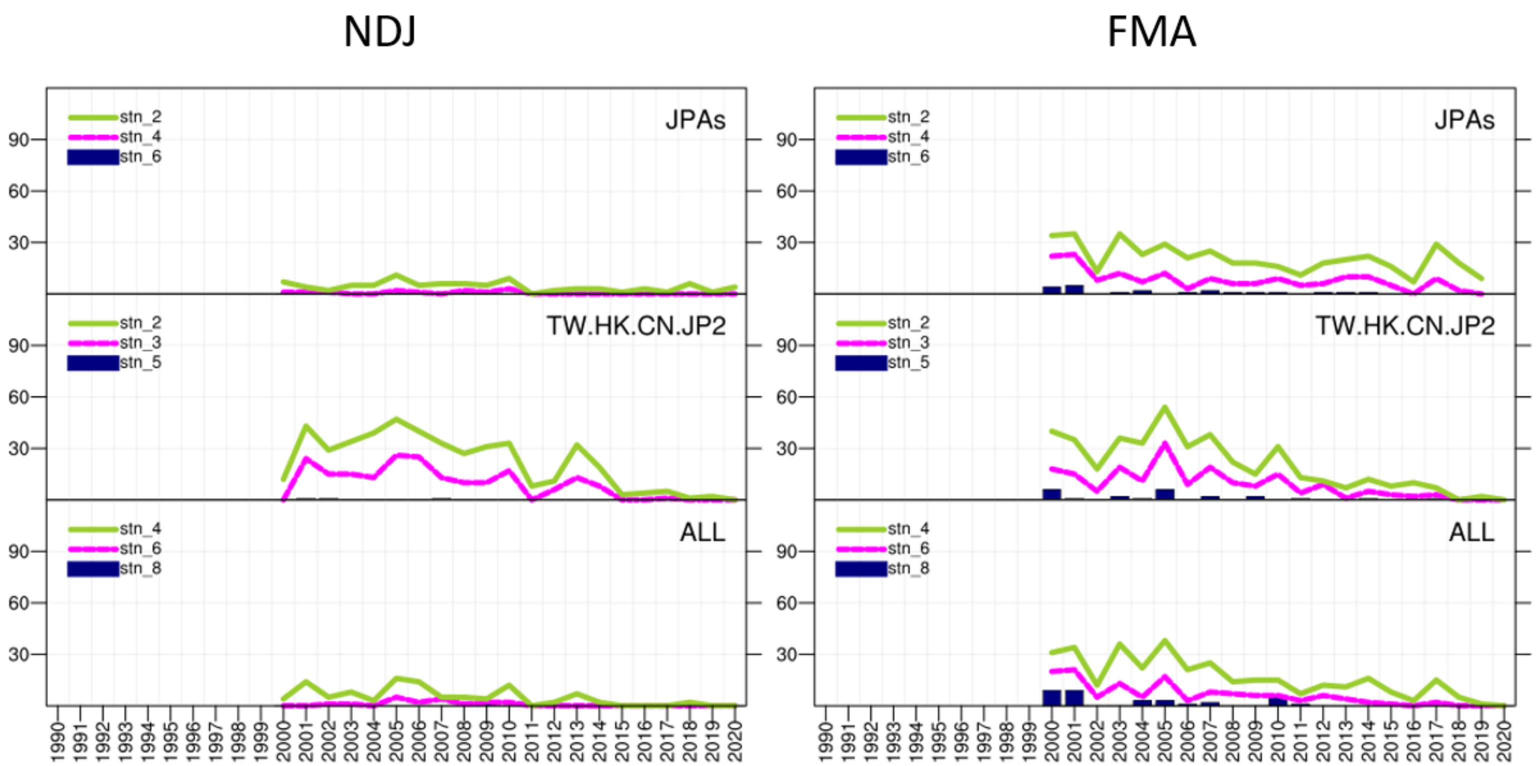

Supplementary Fig. 4 The concurrence of PM_{10} exceedance across the sites. The numbers of days when multiple sites simultaneously exceeded their respective thresholds in (a) winter and (b) spring. Y axis is numbers of day, X axis shows the years of the first month in the cold season. From the top to bottom, panels are for the northern group (6 sites), southern group (5 sites), and all 11 sites. The legends with prefix stn followed by a number indicates the number of sites used in the concurrence calculation.

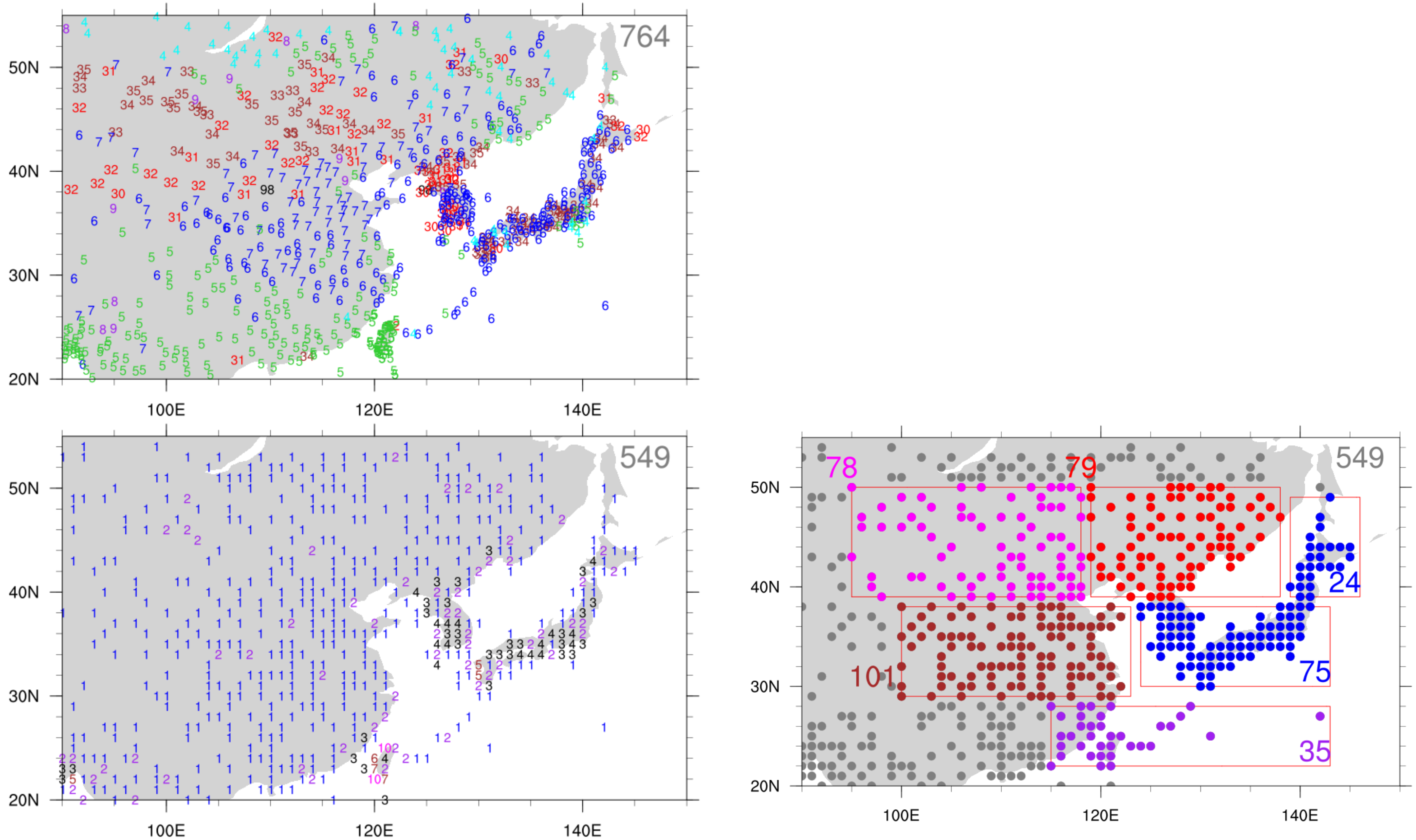

Supplementary Fig. 5 The preprocessing of dust cells. (Upper left) Spatial distribution of the weather stations. The number denotes the highest dust code reported on specific station during our studied period; color-coded based on the value. Gray number of 764 indicate the total numbers of stations. (Bottom left) Remapping/reposition of the weather stations onto a regular grid. The number denote numbers of station in a grid cell, each grid cell is denoted as a dust cell. A number of 1 represents only one station in the specific dust cell, 2 represents there are two stations inside, and so on; color-coded based on the value. Gray number of 549 indicate the numbers of valid dust cell, namely grid cell where at least one station located. (Bottom right) Selected dust cells used for analysis of dust association. The selected dust cells were grouped into 5 sub-regions: 3 continental sub-regions and 2 outflow sub-regions. Numbers with different colors indicate the numbers of dust cell within each sub-region.

Supplementary Table 3 The result of dust association. First two columns are for the 57 dates. The columns GS and GN are the counts of concurrent sites in southern and northern groups; P denotes the defined groups: northern, southern, and broader groups. Within the columns ‘counts on episode date’ and ‘counts within four preceding days’ outlined the counts of the dust cells that meet the conditions that there are dust codes reported (meet our dusty level). We do not have the weather reports for 2018. The references outlined here are those explicitly provided the dates for the investigated dust events; our concurrent dates fell within the specified duration or within one day before or after the given period mentioned in the literature. Footnotes of the table brief on the source and corresponding dates of satellite-based images provided by the NASA Earth Observatory.

						Counts on episode date									Counts within four preceding days of the episode date(s)										
						Continent_all			Outflow_north			Outflow_south			Continent_all			Outflow_north			Outflow_south			Accumulated period	References
		GS	GN	P	Type	4-5	6-9	30+	4-5	6-9	30+	4-5	6-9	30+	4-5	6-9	30+	4-5	6-9	30+	4-5	6-9	30+		
	0305	**5**	**1**	S	**DA**	17	**17**	**4**	0	**10**	**1**	8	0	0											
	0306	**4**	**4**	B	**DA**	10	**28**	**1**	4	**24**	0	10	0	0	53	**46**	**6**	13	**25**	**2**	38	0	0	3/1-4	[10, 14, 15]
	0307	**5**	**4**	B	**DA**	10	**10**	0	8	**40**	0	3	0	0											
	0320	**2**	**6**	B	**DA**	7	**9**	**1**	20	**29**	**1**	7	0	0	56	**19**	**11**	35	**40**	0	30	0	0	3/16-19 & 3/21	[10, 16]
	0322	**2**	**6**	B	**DA**	5	**22**	**4**	5	**31**	**2**	7	**2**	0											
2001	**0413**	**5**	**5**	B	**DA**	3	**8**	0	2	**3**	**1**	10	0	0											
	0414	**5**	**6**	B	**DA**	5	**10**	**1**	12	**10**	0	7	0	0											
	0415	**5**	**5**	B	**DB**	4	**3**	**1**	5	**2**	**1**	11	**1**	0	45	**53**	**18**	58	**62**	**1**	16	0	0	4/9-12	[1, 5, 10, 11, 14] [15, 17, 18, 19]
	0416	**5**	**6**	B	**DB**	13	**2**	**1**	4	**2**	0	6	0	0											
	0417	**3**	**5**	B	**DA**	19	**12**	**3**	11	0	0	7	0	0											
	1127	**5**	**0**	S	**Dr**	9	0	0	0	0	0	9	0	0	48	**2**	0	41	0	**8**	36	**2**	0	11/23-26	**NA**

Supplementary Table 3 (Cont.)

						Counts on episode date									Counts within four preceding days of the episode date(s)										
						Continent_all			Outflow_north			Outflow_south			Continent_all			Outflow_north			Outflow_south			Accumulated	References
		GS	GN	P	Type	4-5	6-9	30+	4-5	6-9	30+	4-5	6-9	30+	4-5	6-9	30+	4-5	6-9	30+	4-5	6-9	30+	period	
2002	0319	5	5	B	DA	5	4	0	0	11	0	9	3	0	25	14	3	36	52	2	11	0	0	3/15-18	[12, 15, 20, 21, 22] [23, 24]
	0320	4	5	B	DA	6	24	19	0	2	0	7	2	0											
	0321	3	6	B	DA	6	26	8	8	17	1	6	0	0											
	0322	2	6	B	DA	7	19	11	10	47	3	5	0	0											
	0401	4	6	B	DA	7	4	0	9	10	0	2	3	0	37	24	0	12	0	0	8	0	0	3/28-31	[20, 24]
	0402	3	5	B	DA	9	2	0	17	9	0	5	3	0											
	0409	1	6	E	DA	7	21	0	9	37	2	2	0	0	4	66	38	12	22	5	13	0	0	4/5-8	[15, 24, 25, 26, 27]
	0410	2	6	B	DA	6	1	0	14	61	0	4	2	0											
	0414	3	5	B	DA	5	17	2	13	7	0	5	0	0	10	6	2	23	27	0	8	0	0	4/11-13	[21, 24]
	0415	3	5	B	DA	6	13	0	14	3	0	4	0	0											
	1218	5	0	S	U	9	0	0	8	0	0	5	0	0	71	0	0	25	0	4	11	0	0	12/14-17	NA
2004	0215	5	2	B	Dr	7	0	0	0	0	0	8	0	0	49	3	0	44	7	7	18	0	0	2/11-14	[15, 20, 27, 28]
	0228	5	0	S	U	3	0	0	5	0	1	11	1	0	30	4	0	27	0	0	18	0	0	2/24-27	NA
	0312	0	6	E	DA	7	0	1	8	4	6	2	0	0	40	34	5	34	23	2	19	1	0	3/8-11	[26, 29]
2005	0319	5	0	S	Dr	5	0	0	0	0	1	6	0	0	20	2	2	21	4	6	27	3	0	3/15-18	[15, 29]
	0415	4	6	B	DA	6	4	0	13	0	1	8	5	0	12	4	2	8	5	8	18	4	0	4/11-14	[28, 30]
	0416	4	6	B	DA	4	4	1	24	7	1	10	0	0											
	0421	4	4	B	DA	0	2	0	7	13	0	7	0	0	14	5	6	41	1	2	19	0	0	4/17-20	[3]

Supplementary Table 3 (Cont.)

						Counts on episode date									Counts within four preceding days of the episode date(s)										
						Continent_all			Outflow_north			Outflow_south			Continent_all			Outflow_north			Outflow_south			Accumulated period	References
		GS	GN	P	Type	4-5	6-9	30+	4-5	6-9	30+	4-5	6-9	30+	4-5	6-9	30+	4-5	6-9	30+	4-5	6-9	30+		
2006	0316	5	0	S	Dr	10	0	0	7	0	0	2	0	0											
	0317	5	2	B	DB	10	7	1	5	0	0	6	1	0	10	6	1	26	3	1	15	0	0	3/12-15 & 3/18	[8, 14, 17, 28, 29]
	0319	5	0	S	DB	8	1	0	10	1	1	16	2	0											
	0329	5	4	B	Dr	5	0	0	8	0	0	9	1	0	25	15	2	43	9	5	10	0	0	3/25-28 & 3/30	[8, 14, 28, 29, 31]
	0331	5	0	S	Dr	7	0	0	1	0	0	7	0	0											
	0418	3	5	B	DA	5	1	1	14	13	0	5	0	0	30	17	2	22	5	7	21	0	0	4/14-17 & 4/19-20	[14, 28, 31]
	0421	5	0	S	DB	5	4	0	1	0	0	7	0	0											
	0425	4	5	B	DA	5	2	0	16	24	0	6	0	0	11	13	1	15	39	6	8	1	0	4/22-24	[8]
2007	0326	2	6	B	Dr	6	0	1	6	0	4	11	0	0	20	1	0	73	1	9	11	0	0	3/22-25	[a]NASA [3/24; 3/31]
2008	0110	5	2	B	U	14	0	0	16	0	3	8	0	0	69	0	0	77	0	11	29	0	0	1/6-9	NA
	0303	5	3	B	DA	7	1	0	10	17	0	9	1	0	26	10	3	22	1	4	27	0	0	2/28-3/2	[32]
	0304	5	1	S	Dr	8	0	0	1	4	0	7	2	0											
	0427	4	4	B	DB	13	3	0	24	0	1	10	0	0											
	0429	0	6	E	DB	10	2	2	24	0	0	5	0	0	71	8	0	77	0	9	32	0	0	4/23-26 & 4/28	[33] [b]NASA [4/25,28]
	0430	0	6	E	DB	10	3	1	35	0	2	5	0	0											
	1210	0	6	E	Dr	10	0	0	8	0	11	3	0	0	38	4	0	10	4	3	13	0	0	12/6-9	NA

[a&b]The NASA images for East Asian dust activities (the URLs and their respective dates, lased accessed on June 8, 2023).
[a]NASA [3/24]: Dust storm in Northern China on March 24, 2007 (https://earthobservatory.nasa.gov/images/18175/dust-storm-in-northern-china).
[a]NASA [3/31]: Dust over Eastern China on March 31, 2007 (https://earthobservatory.nasa.gov/images/18217/dust-and-clouds-over-eastern-china).
[b]NASA [4/25]: Dust storm over Eastern China on April 25, 2008 (https://earthobservatory.nasa.gov/images/19841/dust-storm-over-eastern-china).
[b]NASA [4/28]: Dust storm in Eastern China on April 28,2008 (https://spaceref.com/status-report/nasa-modis-image-of-the-day-april-28-2008-dust-storm-in-eastern-china/)

Supplementary Table 3 (Cont.)

						Counts on episode date									Counts within four preceding days of the episode date(s)										
						Continent_all			Outflow_north			Outflow_south			Continent_all			Outflow_north			Outflow_south			Accumulated	References
		GS	GN	P	Type	4-5	6-9	30+	4-5	6-9	30+	4-5	6-9	30+	4-5	6-9	30+	4-5	6-9	30+	4-5	6-9	30+	period	
2009	0317	1	6	E	DA	10	5	3	15	29	1	6	0	0	22	4	2	11	9	3	15	0	0	3/13-16	[3, 7, 8]
	1226	4	4	B	DA	14	0	1	23	16	2	12	1	0	59	4	2	43	0	11	21	0	0	12/22-25	[7, 34, 35, 36]
2010	0320	1	6	E	DA	8	33	2	28	0	0	8	0	0											[2, 3, 4, 29, 37] [38, 39]
	0322	5	1	S	DA	10	22	1	2	0	0	16	8	0	35	22	7	49	50	8	33	6	1	3/16-19 & 3/21	
	0323	5	0	S	DA	6	3	0	4	2	1	6	4	0											
2011	0410	2	6	B	DB	5	1	0	13	0	2	6	0	0	22	7	0	11	0	5	22	0	0	4/6-9	[6]
2012	0402	5	3	B	Dr	7	0	0	3	0	1	4	0	0	15	4	1	20	0	3	21	1	0	3/29-4/1	[3, 9, 29]
2013	0416	0	6	E	Dr	9	0	0	7	0	0	4	0	0	36	3	3	9	0	8	11	0	0	4/12-15	[c]NASA [4/17]
2014	0225	1	6	E	U	31	1	0	38	0	2	3	0	0	105	0	0	46	0	5	18	0	0	2/21-24	[d]NASA [4/23]
2015	0218	5	0	S	U	31	0	0	12	0	0	11	0	0	110	1	1	33	0	4	25	0	0	2/14-17	NA
	0418	1	6	E	DB	10	2	0	3	0	0	2	0	0	83	17	3	27	3	1	19	0	0	4/12-17	[13]
2018	0407	5	2	B	D																				[3, 40, 41]

[c&d]The NASA images for East Asian dust activities (the URLs and their respective dates, lased accessed on June 8, 2023).
[c]NASA [4/17]: Dust storm in China and Mongolia on April 17, 2013 (https://earthobservatory.nasa.gov/images/80940/dust-storm-in-china-and-mongolia)
[d]NASA [4/23]: Dust wall over northern China on April 23, 2014 (https://earthobservatory.nasa.gov/images/83554/chinas-great-wall-of-dust)

REFERENCES

[1] Bates, T. S. et al. Marine boundary layer dust and pollutant transport associated with the passage of a frontal system over eastern Asia. J. Geophys. Res. 109, D19S19 (2004).

[2] Huang, Z. J. et al. Short-cut transport path for Asian dust directly to the Arctic: a case study, Environ. Res. Lett. 10, 114018 (2015).

[3] Jeong, G. Y. Mineralogy and geochemistry of Asian dust: dependence on migration path, fractionation, and reactions with polluted air. Atmos. Chem. Phys., 20, 7411 – 7428 (2020).

[4] Li, J., Han, Z. & Zhang, R. Model study of atmospheric particulates during dust storm period in March 2010 over East Asia. Atmos. Environ. 45, 3954 – 3964 (2011).

[5] Liu, M. et al. A high-resolution numerical study of the Asian dust storms on April 2001. J. Geophys. Res. 108, 8653 (2003).

[6] Moreno, T. et al. Daily and hourly chemical impact of springtime transboundary aerosols on Japanese air quality. Atmos. Chem. Phys. 13, 1411 – 1424 (2013).

[7] Sugimoto, N. et al. Analysis of dust events in 2008 and 2009 using the lidar network, surface observations and the CFORS model. Asia-Pacific J Atmos Sci 49, 27 – 39 (2013).

[8] Tsai, F. & Chen, W.-N. Comparison of the Synoptic Environments Conducive to Eastward versus Southeastward Transport of Asian Dust Events. Advances in Meteorology 2014, 467659 (2014).

[9] Tsedendamba, P. et al. Northeast Asian Dust Transport: A Case Study of a Dust Storm Event from 28 March to 2 April 2012. Atmosphere 10, 69 (2019).

[10] Uno, I. et al. Numerical study of Asian dust transport during the springtime of 2001 simulated with the chemical weather forecasting system (CFORS) model. J. Geophys. Res. 109, D19S24 (2004).

[11] Wang, K. Y. Long-range transport of the April 2001 dust clouds over the subtropical East Asia and the North Pacific and its impacts on ground-level air pollution: A Lagrangian simulation. J. Geophys. Res. 112, D09203 (2007).

[12] Zhao, X., Wang, Z., Zhuang, G. & Pang, C. Model study on the transport and mixing of dust aerosols and pollutants during an Asian dust storm in March 2002. Terr. Atmos. Oceanic Sci. 18, 437 – 457 (2007).

[13] Zhao, X., Huang, K., Fu, J. S. & Abdullaev, S. F. Long-range transport of Asian dust to the Arctic: identification of transport pathways, evolution of aerosol optical properties, and impact assessment on surface albedo change. Atmos. Chem. Phys. 22, 10389 – 10407 (2020).

[14] Lee, Y. C., Yang, X. & Wenig, M. Transport of dusts from East Asian and non-East Asian sources to Hong Kong during dust storm related events 1996-2007. Atmos. Environ. 44, 3728-3738 (2010).

[15] Liu, C.-M., Young, C.-Y. & Lee, Y.-C. Influence of Asian dust storms on air quality in Taiwan. Sci. Total Environ. 368, 884 – 897 (2006).

[16] Ro, C.-U., Hwang, H., Kim, H., Chun, Y., & van Grieken, R. Single-particle characterization of four "Asian dust" samples collected in Korea, using low-Z particle electron probe X-ray microanalysis. Environ. Sci. Technol. 39, 1409 – 1419 (2005).

[17] Lin, C.-Y. et al. Long-range transport of Asian dust and air pollutants to Taiwan. Terr. Atmos. Oceanic Sci. 15, 759 – 784 (2004).

[18] Tsai, F., Chen, G. T. J., Liu, T. H., Lin, W. D. & Tu J. Y. Characterizing the transport pathways of Asian dust. J. Geophys. Res., 113, D17311 (2008).

[19] Chen, S. J. et al. Characteristics of particles sampled in southern Taiwan during the Asian dust storm periods in 2000 and 2001. Atmos. Environ. 38, 5925 – 5934 (2004).

[20] Nee, J. B., Chiang, C.-W., Hu, H.-L., Hu, S.-X., Yu, J.-Y. Lidar measurements of Asian dust storms and dust cloud interactions. J. Geophys. Res. 112, D15202 (2007).

[21] Lee S., Chun Y., Nam J.-C., Park S.-U. & Lee E.-H. Estimation of dry deposition during Asian dust events in spring of 2002. J. Meteorol. Soc. Jpn. 83A, 241 – 254 (2005).

[22] Ma, C.-J., Tohno, S. & Kasahara M. A case study of the size-resolved individual particles collected at a ground-based site on the west coast of Japan during an Asian dust storm event. Atmos. Environ., 39, 739 – 747 (2005).

[23] Park, S.-U. & In H.-J. Parameterization of dust emission for the simulation of the yellow sand (Asian dust) event observed in March 2002 in Korea. J. Geophys. Res. 108, 4618 (2003).

[24] Shao, Y. & Wang, J. A climatology of Northeast Asian dust events. Meteorol. Z. 12, 187 – 196 (2003).

[25] Lee, B.-K., Lee, H. K. & Jun, N.-Y. Analysis of regional and temporal characteristics of PM10 during an Asian dust episode in Korea, Chemosphere, 63, 1106 – 1115 (2006).

[26] Lim, J. Y. & Chun Y. The characteristics of Asian dust events in Northeast Asia during the springtime from 1993 to 2004. Global Planet. Change 52, 231 – 247 (2006).

[27] Lin, C.-Y. et al. Impact of different transport mechanisms of Asian dust and anthropogenic pollutants to Taiwan. Atmos. Environ. 60, 403 – 418 (2012).

[28] Liu, T.-H. et al. Southeastward transport of Asian dust: source, transport and its contributions to Taiwan. Atmos. Environ. 43, 458 – 467 (2009).

[29] Park, S.-B., Cho, J.-A., Park, S. S., Koo, J.-H. & Lee, Y. G. A Possible Linkage between Dust Frequency and the Siberian High in March over Northeast Asia. Atmosphere 12, 176 (2021).

[30] Zhang, R., Han, Z., Cheng, T. & Tao, J. Chemical properties and origin of dust aerosols in Beijing during springtime. Particuology, 7, 61 – 67 (2009).

[31] Dong, X. et al. Analysis of the Co-existence of Long-range Transport Biomass Burning and Dust in the Subtropical West Pacific Region. Sci Rep 8, 8962 (2018).

[32] Chu, H. J., Yu, H. L. & Kuo, Y. M. Identifying spatial mixture distributions of PM2.5 and PM10 in Taiwan during and after a dust storm. Atmos. Environ. 54, 728 – 737 (2012).

[33] Zhang, Y., Cai, Y.J., Yu, F., Luo, G. & Chou, C.C.K. Seasonal Variations and Long-term Trend of Mineral Dust Aerosols over the Taiwan Region. Aerosol Air Qual. Res. 21, 200433 (2021).

[34] Kang, J.-Y., Tanaka, T. Y., Mikami, M. & Yoon, S.-C. A numerical study of the effect of frozen soil on dust emission during an East Asian dust event in December 2009. Asia-Pacific J Atmos Sci 49, 57 – 65 (2013).

[35] Lee, H., Kim, J.E. & Chun, Y. The comparison of two severe Hwangsa (Asian dust) cases of spring and winter in Seoul, Korea. Asia-Pacific J Atmos Sci 49, 49 – 56 (2013).

[36] Park, S.U., Choe, A. & Park, M.S. A simulation of Asian dust events observed from 20 to 29 December 2009 in Korea by using ADAM2. Asia-Pacific J Atmos Sci 49, 95 – 109 (2013).

[37] Bian, H. et al. Analysis of a Severe Dust Storm Event over China: Application of the WRF-Dust Model. Aerosol Air Qual. Res. 111, 419 – 428 (2011).

[38] Hsu, S. C. et al. Dust transport from non-East Asian sources to the North Pacific, Geophys. Res. Lett. 39, L12804, doi:10.1029/2012GL051962 (2012).

[39] Hsu, S.-C. et al. A super Asian dust storm over the East and South China Seas: Disproportionate dust deposition. J. Geophys. Res. Atmos. 118, 7169 – 7181 (2013).

[40] Kong, S.S.-K. et al. Sensitivity analysis of the dust emission treatment in CMAQv5.2.1 and its application to long-range transport over East Asia. Atmos. Environ. 257, 118441 (2021).

[41] Yang, H. et al. Impacts of transboundary dust transport on aerosol pollution in the Western Yangtze River Delta Region, China: Insights gained from ground-based lidar and satellite observations. Earth Sp. Sci. 8, e2020EA001533 (2021).